Simulation of Effects of Nafion Loading in Catalyst Layer on Performance of Proton Exchange Membrane Fuel Cells

CHIN-HSIANG CHENG
Department of Aeronautics and Astronautics
National Cheng Kung University
Tainan, Taiwan 70101, R.O.C.

Hung-Hsiang Lin and Guang-Jer Lai
Department of Mechanical Engineering
Tatung University
Taipei, Taiwan 10451, R.O.C.

Abstract: - The present study is concerned with the influence of Nafion loading in the catalyst layers on the behavior of a proton exchange membrane fuel cell (PEMFC). Numerical simulation is performed to predict the Nafion loading effects. Meanwhile, change in the performance of the PEMFC accompanying the variations of geometric parameters is also investigated. In this study, a self-developed code, which is used to deal with the volume fractions of Nafion loaded, solid catalyst particles, and void space inside the catalyst layers, is incorporated with a three-dimensional computational fluid dynamics code, which is capable of dealing with the three-dimensional mass, momentum, and species transport phenomena as well as the electron-transfer process taking place in the PEMFC. Part of the numerical results is compared with the experiments, and a close agreement between the predictions and the experiments has been found.
Key-Words: - Nafion loading, PEMFC, Parametric study, Prediction, Experiment

1 Introduction

Fuel cells are an important technology for a potentially wide variety of applications including auxiliary power, transportation power, and stationary power for buildings and other distributed generation applications. These applications are encountered in a large number of industries worldwide.

In the electrochemical reactions of the proton exchange membrane fuel cells (PEMFC), hydrogen at the anode provides protons, freeing electrons in the process that must pass through an external circuit to reach the cathode. The protons, which remain solvated with a certain number of water molecules, diffuse through the membrane to the cathode to react with oxygen and the returning electrons. Water is subsequently produced at the cathode. In a PEMFC, Nafion is used as the membrane placed between the anode and the cathode. Furthermore, it is also employed as an important component of the active layer in the catalyst layer. The content of Nafion in the catalyst layers affects simultaneously the gas permeability, the catalytic activity and the ionic resistance. Hence, an optimal Nafion content in the catalyst layer is definitely desired for good performance.

Based on the existing studies, it may be noted that even though experiments for the optimal Nafion content in the catalyst layers have been performed well by a groups of authors [1-5], the theoretical information for the effects of Nafion loading is relatively lacking. Reliable information about the fuel cell behavior may be collected by experimental or numerical methods. So far, unfortunately, only a limited number of theoretical reports, for example, Refs.[6,7], have been presented. Among the very few theoretical works, Song, et al.[6] proposed an optimization problem for the cathode catalyst layer performance by assuming that the Nafion content and Pt loading are uniformly distributed in the cathode catalyst layer. From this, the optimal Nafion content, Pt loading, and layer thickness were determined.

With the help of theoretical study, the basics of the improvement of fuel cell performance by Nafion loading might be clarified and the optimal Nafion content could be determined. In these circumstances, the present study is aimed to investigate the influence of Nafion loading in the catalyst layers on the behavior of a proton exchange membrane fuel cell by numerical simulation. In this study, a self-developed code, which is used to deal with the volume fractions of Nafion loaded, solid catalyst particles, and void space inside the catalyst layers, is incorporated with a three-dimensional computational fluid dynamics code, which is capable of dealing with the three-dimensional mass, momentum, and species transport phenomena as well as the electron- and proton-transfer process taking place in the PEMFC.

Schematic of a single-cell PEMFC with parallel straight channels on the carbon plates for both the anode and the cathode is shown in Fig.1. The single-cell PEMFC consists of a carbon plate, a gas diffusion layer (GDL), a catalyst layer, for each of the anode and the cathode, and a PEM membrane at the center. Here the physical and geometrical parameters of the cell shown in this figure may be divided into two groups: the fixed and the varied parameters. For these fixed parameters, their values are kept constant throughout the study. On the other hand, as mentioned earlier, the volume fraction of Nafion in the catalyst layer ($\varepsilon_{N,Cat}$), the volume fraction of void space in the catalyst layer ($\varepsilon_{V,Cat}$), the gas channel width (l_C), the gas channel height (h), and the thickness of the gas diffusion layer (t_{GDL}), are regarded as major factors and are varied in this study in order to evaluate their effects. These parameters are referred to as the varied parameters.

2 Theoretical Analysis and Numerical Methods

The following assumptions are made in prior to the derivation of the governing equations:

1. The fuel cell operates steadily;
2. The gas flows in the gas channels and the porous layers are laminar and compressible, and effects of buoyancy on the flow motion are negligible;
3. Thermodynamic and electrochemical properties of the gases and the solid materials of the fuel cell components are assumed constant;
4. The operating pressure and temperature are uniform and constant in the solution domain;
5. The gas diffusion layers and the catalyst layers are homogeneous, isotropic porous media;
6. Owing to high ohmic resistance of the membrane, the interface between the catalyst layer and the membrane is assumed to be insulated against electrons;
7. Water exists in the entire fuel cell only in vapor phase, and no phase change process is taken into consideration.

2.1 Theoretical Model

The conservation equations along with the property equations are solved by adopting a finite-volume scheme on structured grids within the framework of the commercial computational fluid dynamics code (CFD-ACE+). In addition, the theoretical model is applied to evaluating the influence of Nafion loading at various combinations of the volume fractions of Nafion loaded, solid catalyst particles, and void space in the catalyst layers.

2.1.1 Nafion loading (catalyst)

As mentioned earlier, Nafion is an electronic insulator. Hence, when it is introduced into the catalyst layer, it decreases the electronic conductivity of the catalyst layer. However, on the other hand, since it is a good conductor for the hydrogen protons, Nafion loading can elevate the ionic conductivity of the catalyst layers. Besides, the introduction of Nafion into the catalyst layers changes simultaneously the porosity and the gas permeability of the layers so that it affects the transport of the gas species. As Nafion is loaded, total volume of the catalyst layer (υ_t) may be divided into three major portions, namely, the volume occupied by the solid catalyst particles (υ_S), the volume occupied by Nafion (υ_N), and the volume of the void space(υ_V). The volume fractions of the three portions are denoted by $\varepsilon_{S,Cat}$, $\varepsilon_{N,Cat}$, and $\varepsilon_{V,Cat}$, respectively, and are defined as

$$\varepsilon_{S,Cat} = \frac{\upsilon_S}{\upsilon_t} \tag{1a}$$

$$\varepsilon_{N,Cat} = \frac{\upsilon_N}{\upsilon_t} \tag{1b}$$

and

$$\varepsilon_{V,Cat} = 1 - \varepsilon_{S,Cat} - \varepsilon_{N,Cat} \tag{1c}$$

It is noted that the present model dose not include the effects of heat and liquid water accumulation. A more powerful model will absolutely be desired when necessary. However, the simplification of the model is acceptable, given that the Nafion loading is emphasized rather than the complexity of the model

2.1.2 Solution domain and boundary conditions

For the pattern of straight parallel channels shown in Fig.1, as the number of gas channels is large enough, a periodic transport phenomenon is expected to develop from channel to channel. Thus, one only needs to deal with the solution domain of a single module indicated by the dashed lines. In this study, the width of a module (l_P) is set to be 1 mm. Therefore, for the faces of solution domain at x = 0 and x = 1 mm, a symmetric boundary condition for $\vec{U}$, Y, ϕ, and φ is prescribed.

Solid walls of the gas channels or the carbon plates are impermeable, and hence, on the solid walls, $\frac{\partial Y_i}{\partial n} = 0$ and $\vec{U}$ =0. In addition, since both the gas channels and the membrane are insulators against electrons; at the boundaries of these two components, the normal gradient of the electric potential (ϕ) is vanished. Furthermore, the ionic conduction takes place only inside the catalyst layer and proton

exchange membrane, and the protons are not allowed to transfer into other components; therefore, on the faces of the catalyst layer and the membrane the normal gradient of phase potential is assigned to be zero.

As to the inlet conditions, the inlet velocities for the anode gas (hydrogen) and the cathode gas (air) in the gas channel, V_a and V_c, are fixed at 0.3 and 0.5 m/s, respectively. Note that both the fuel and the oxidant gases enter the fuel cell at 100% relative humidity. On the other hand, for the boundary conditions at the exit, it is assumed that the flow becomes fully developed downstream. Thus, the exit boundary conditions may be described as

$$u = w = \frac{\partial v}{\partial y} = \frac{\partial Y_i}{\partial y} = \frac{\partial \phi}{\partial y} = \frac{\partial \varphi}{\partial y} = 0 \qquad (2)$$

2.2 Numerical Methods

A self-developed code has been built for calculating the values of the properties of the catalyst layers, including the effective electronic conductivity, the effective ionic conductivity, and effective mass diffusivity of gas species (σ_{Cat}^{eff}, Γ_{Cat}^{eff}, and D_i^{eff}) for various Nafion loading conditions. The Nafion loading condition is specified by adjusting the values of volume fractions of Nafion loaded, solid catalyst particles, and void space inside the catalyst layers ($\varepsilon_{N,Cat}$, $\varepsilon_{S,Cat}$, and $\varepsilon_{V,Cat}$). The self-developed code is incorporated with the computational fluid dynamics code. Through a Python-interface connection between the two codes, the message of any change in the Nafion content is firstly used by the self-developed code to update the values of the properties of the catalyst layer, and then the updated values of the catalyst layer properties can be transmitted automatically to the computational fluid dynamics code in order for solution of the three-dimensional transport phenomena taking place in the PEMFC. When necessary, the CFD code solutions may also be sent back to the self-developed code through the connection for successive computation or further evaluation. The connection between the two codes is shown in Fig. 2.

The average current density (**I**) of fuel cells is calculated by integration of local current density distribution on the carbon plate surface at $z = 0$ divided by the carbon plate surface area as

$$\mathbf{I} = \frac{1}{A}\int_0^A i_s \cdot dA \qquad (3)$$

where i_s is the local current density on the carbon plate surface, and A is the carbon plate surface area. In the mean time, the gas channel width fraction (Λ) is defined by the ratio of the gas channel width (l_C) to the width of a module (l_P), which is

$$\Lambda = l_C / l_P \qquad (4)$$

3 Experiments

A single-cell fuel cell module with cross-sectional area of 22×22 cm^2 and active area of 14×14 cm^2 has been installed and tested to partly confirm the numerical predictions yielded by the commercial computational fluid dynamics code. The purpose of the experiments is simply to test the validity of the CFD code; therefore, Nafion is not yet introduced into the catalyst layers of the MEA. The operating and geometrical conditions in simulation are consistent with the experimental module. Two composite graphite plates of 3-mm thickness are used as the flow fields and current conductors. A 5-layer membrane exchange assembly (MEA) provided by Dupont Inc. is placed at the center between the two composite graphite plates. The membrane used in this MEA is Nafion® 112 and the gas diffusion layers are made of carbon fiber paper. Before entering the channels, the fuel and oxidant gases are humidified to maintain at 100% relative humidity and 80 ℃ temperature.

In addition, to obtain the polarization curves with the fuel cell, a performance test system has also been setup. In the experiments, the volumetric flow rates of the hydrogen and the air are typically maintained at 1500 sccm and 2500 sccm, corresponding to V_a = 0.3 m/s and V_b = 0.5 m/s, respectively. The fuel cell temperature is maintained at 343 K.

Figure 3 shows a comparison between the numerical predictions and the experiment data for the polarization curves of the single-cell fuel cell module without Nafion loading. The operating conditions have been described in the preceding section. It is observed that the numerical predictions closely agree with the experiments, especially as **I** < 3800 A/m^2. The difference between the two sets of data becomes appreciable only in the high-current-density regime. In this regime, the experimental data appear to experience a greater drop in the operating voltage than the predicted. The greater voltage drop is attributed to the concentration loss due to insufficient H_2 supply in experiments, which is remarkable in the high current density situations. In Fig. 3, it is found that at **V** = 0.7 Volt the numerical and the experimental data for the current density are in close agreement (at approximately 2500 A/m^2). Thus, the typical value of the operating voltage of the fuel cell is fixed at 0.7 Volt in the present study to evaluate the Nafion loading effects.

4 Results and Discussion

Given the operating conditions of **V**=0.7 Volt, ε_{GDL}=0.5, $\varepsilon_{S,Cat}$=0.588, t_{GDL}=5×10^{-4} m, t_m=1.76×10^{-4} m, h=1×10^{-3} m, and Λ=0.5, one may examine the dependence of power density of the PEMFC (**P**) on the volume fraction of Nafion in the catalyst layer ($\varepsilon_{N,Cat}$). The predicted results are plotted in Fig.4. It is clearly seen that the magnitude of the power density first increases with $\varepsilon_{N,Cat}$ to reach its optimal value of approximately 1812 W/m^2 at $\varepsilon_{N,Cat}$=0.3, and then descends when the value of $\varepsilon_{N,Cat}$ over the optimal one. The finding basically agrees with the observation of Qi, et al. [5] who found that 30% Nafion content leads to optimal performance for the fuel cell.

The data shown in Fig.4 are collected as the volume fraction of solid catalyst particles in the catalyst layer ($\varepsilon_{S,Cat}$) is fixed at 0.588. On the other hand, what plotted in Fig.5 is the information concerning the dependence of power density on $\varepsilon_{N,Cat}$ at a constant volume fraction of void space in the catalyst layer ($\varepsilon_{V,Cat}$). Results proved in Fig.5 illustrates that in this case the maximum power density can be yielded when the volume fraction of Nafion in the catalyst layer is maintained at 0.45.

Figure 6 shows the variation of power density with the volume fraction of void space in the catalyst layer for **V**=0.7 Volt, ε_{GDL}=0.5, $\varepsilon_{N,Cat}$ =0.3, l_C=5×10^{-4} m, t_{GDL}=3×10^{-4} m, t_m=1.76×10^{-4} m, h=1×10^{-3} m and Λ=0.5. The volume fraction of void space in the catalyst layer ($\varepsilon_{V,Cat}$) is also referred to as the porosity of the catalyst layer. An increase in $\varepsilon_{V,Cat}$ is favorable for sufficient gas supply; however, it reduces the ionic and the electronic conduction. For the case considered in this figure, it is observed that the optimal power density is reached at $\varepsilon_{V,Cat}$=0.125.

Figure 7 further conveys the effects of gas channel width fraction (Λ) on the performance of the fuel cell at **V**=0.7 Volt, ε_{GDL}=0.5, $\varepsilon_{V,Cat}$=0.112, $\varepsilon_{N,Cat}$ =0.3, t_{GDL}=3×10^{-4} m, t_m=1.76×10^{-4} m, and h=1×10^{-3} m. It is observed that indeed the channel width fraction has subtle influence on the cell performance. Larger channel width fraction may enhance the gases transport as well as the chemical reaction in the catalyst layer; however, a larger channel width leads to narrower ribs and hence results in an increase in the ohmic impedance. With these two opposing effects, there must exist an optimal value of gas channel width fraction, at which the performance reaches a peak value. In Fig. 7, the results show that the largest power of 1816 W/m^2 is obtained at the optimal gas channel width fraction of Λ=0.4 under the conditions considered in this case.

Power density as a function of the height of gas channels (h) is shown in Fig.8, for **V**=0.7 Volt, ε_{GDL}=0.5, $\varepsilon_{V,Cat}$=0.112, $\varepsilon_{N,Cat}$ =0.3, l_C=5×10^{-4} m, t_{GDL}=3×10^{-4} m, t_m=1.76×10^{-4} m, and Λ=0.5. Mass flow rates of the reactant gases can be elevated by increasing the height of gas channels, so as to provide more gases for reaction; however, higher channels may also lead to a slight increase in the ohmic impedance. As a result, the optimal fuel cell performance can be found at h=1.0 mm. As the height of the gas channels becomes greater than 1.0 mm, the fuel cell performance will be slightly reduced again.

Plotted in Fig.9 is the variation in the power density with the thickness of gas diffusion layer (t_{GDL}) for **V**=0.7 Volt, ε_{GDL}=0.5, $\varepsilon_{V,Cat}$=0.112, $\varepsilon_{N,Cat}$ =0.3, l_C=5×10^{-4} m, t_m=1.76×10^{-4} m, h=1×10^{-3} m and Λ=0.5. A thicker gas diffusion layer may allow the gas to disperse uniformly in the entire gas diffusion layer; however, it also tends to increase the electric resistance against the conduction of electrons. It is seen that the optimal performance of the fuel cell is 1828W/m^2 at t_{GDL}=200μm. In addition, the porosity of the gas diffusion layer (ε_{GDL}) is also one of the major factors affecting the fuel cell performance. Similarly, an increase in ε_{GDL} is favorable for sufficient gas supply; however, it tends to increase the electric resistance. For the case at **V**=0.7 Volt, $\varepsilon_{V,Cat}$=0.112, $\varepsilon_{N,Cat}$ =0.3, l_C=5×10^{-4} m, t_{GDL}=3×10^{-4} m, t_m=1.76×10^{-4} m, h=1×10^{-3} m and Λ=0.5, the results shown in Fig.10 illustrate that the peak value of the power density can be achieved at ε_{GDL} = 0.3.

5 Conclusions

This study is concerned with the Nafion loading effects by numerical simulation using a full-cell three-dimensional numerical model. In addition, change in the performance of the PEMFC accompanying various combinations of geometric parameters is also investigated.

A self-developed code has been built for calculating the values of the properties of the catalyst layers, including the effective electronic conductivity, the effective ionic conductivity, and effective mass diffusivity of gas species (σ_{Cat}^{eff}, Γ_{Cat}^{eff}, and D_i^{eff}) for various Nafion loading conditions. The self-developed code is incorporated with a computational fluid dynamics code through a Python-interface connection to deal with the three-dimensional mass, momentum, and species transport phenomena as well as the electron-transfer process taking place in the PEMFC.

For the particular cases considered in this study, results show that the optimal parameters which lead to a higher fuel cell power density are: $\varepsilon_{N,Cat}$=0.3 to 0.45; $\varepsilon_{V,Cat}$=0.125; Λ=0.4; h=1.0 mm; and t_{GDL}=200μm. Note that the suggested optimal parameters are obtained under the base case conditions considered in the present study. When the conditions are changed, the optimal values of these parameters may be altered.

6 References:

[1] C.C. Boyer, R.G. Anthony, and A.J. Appleby, Design equations for optimized PEM fuel cell electrode, *Journal of Applied Electrochemistry*, Vol.30, 2000, pp. 777-786.

[2] E. Passalacqua, F. Lufrano, G. Squadrito, A. Patti, and L. Giorgi, Influence of the structure in low-Pt loading electrodes for polymer electrolyte fuel cells, *Electrochim. Acta*, Vol. 43, 1998, pp. 3665-3673.

[3] E. Passalacqua, F. Lufrano, G. Squadrito, A. Patti, and L. Giorgi, Nafion content in the catalyst layer of polymer electrolyte fuel cells: effects on structure and performance, *Electrochim. Acta*, Vol. 46, 2001, pp. 799-805.

[4] E. Antolini, L. Giorgi, A. Pozio, and E. Passalacqua, Influence of Nafion loading in the catalyst layer of gas-diffusion electrodes for PEFC, *Journal of Power Sources*, Vol. 77, 1999, pp. 136-142.

[5] Z. Qi, and A. Kaufman, Low Pt loading high performance cathodes for PEM fuel cells, *Journal of Power Sources*, Vol.113, 2003, pp. 37-43.

[6] D. Song, Q. Wang, Z. Liu, T. Navessin, M. Eikerling, and S. Holdcroft, Numerical optimization study of the catalyst layer of PEM fuel cell cathode, *Journal of Power Sources*, Vol. 126, 2004, pp. 104-111.

[7] D. Song, Q. Wang, Z. Liu, T. Navessin, M. Eikerling, Z. Xie, T. Navessin, and S. Holdcroft, A method for optimizing distributions of Nafion and Pt in cathode catalyst layers of PEM fuel cells, *Electrochim. Acta*, Vol. 50, 2005, pp. 3347-3358.

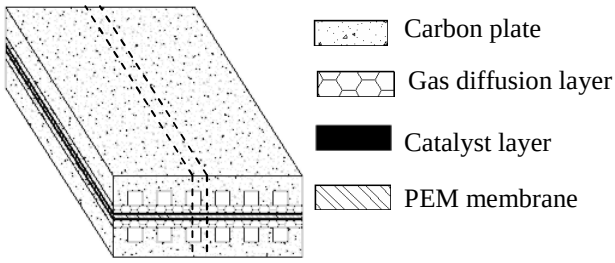

(a) Single cell with parallel straight channels

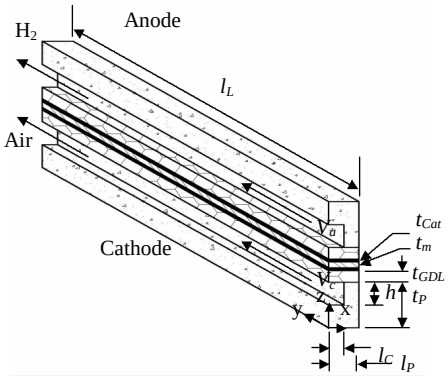

(b) Flow channel geometry

Fig.1 Schematic of a single-cell proton exchange membrane fuel cell.

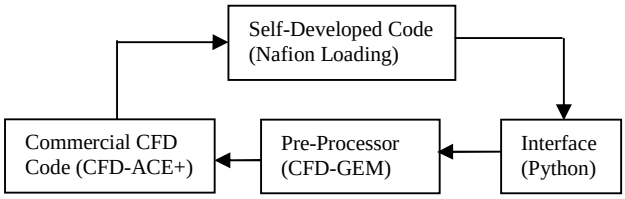

Fig.2 Connection between self-developed and commercial codes.

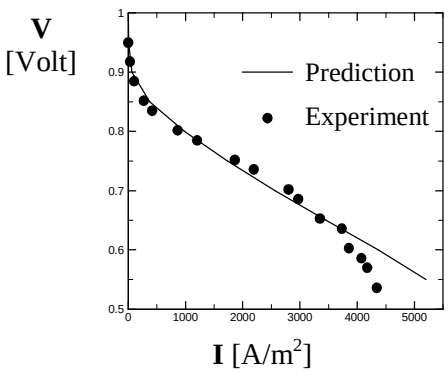

Fig.3 Polarization curves: comparison between predictions and experiments.

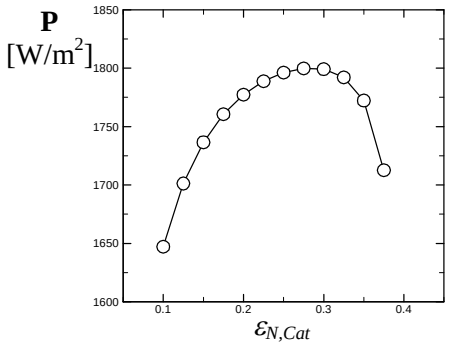

Fig.4 Power density as a function of volume fraction of Nafion in catalyst layer, at $\varepsilon_{S,Cat}$ = 0.588.

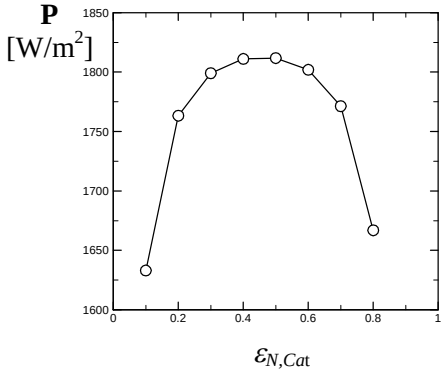

Fig.5 Power density as a function of volume fraction of Nafion in catalyst layer, at $\varepsilon_{V,Cat}$=0.112.

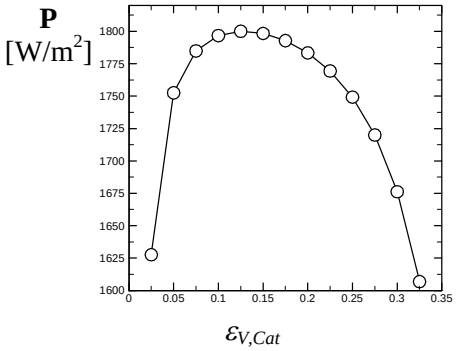

Fig.6 Power density as a function of volume fraction of void space in catalyst layer.

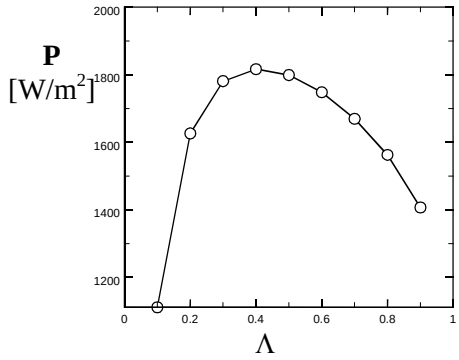

Fig.7 Power density as a function of channel width fraction.

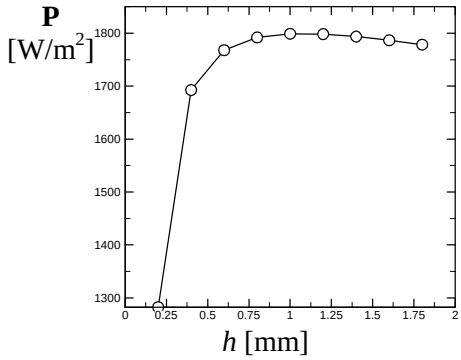

Fig.8 Power density as a function of height of gas channels.

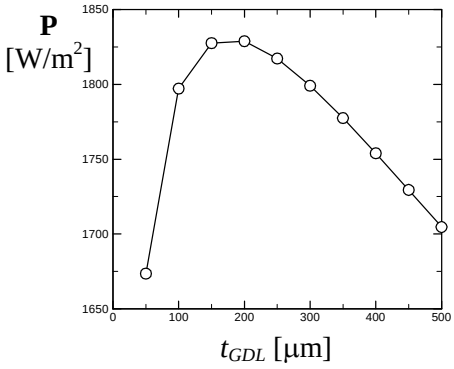

Fig.9 Power density as a function of thickness of gas diffusion layer.

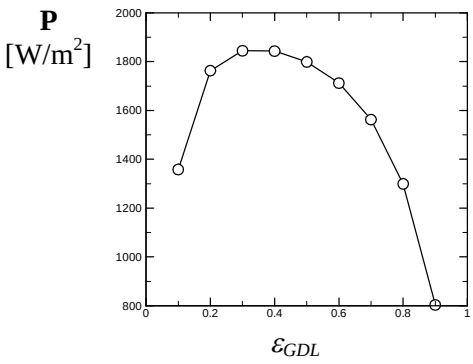

Fig.10 Power density as a function of porosity of gas diffusion layer.